(Dated: December 2022)

I. INTRODUCTION

Modelling the behavior of nuclei across the nuclear landscape is one of the overarching goal of nuclear physics. An avenue for better predicting the behavior of exotic nuclei is to study nuclear reactions. In order to simplify the many-body problem of a nuclear reaction, we implement optical potentials which reduce the many-body problem to just a few-body problem by using an effective interaction that describes the nuclear reaction. Optical potentials generally exhibit three important features: they are nonlocal, energy dependent, and complex (if the reaction involves the excitation of the target or projectile). Studying optical potentials are important in calculating scattering cross sections, and comparing the theoretically calculated cross sections to experimental data allows us to better understand the behaviors of exotic nuclei. However, to accurately calculate the cross section, we need input from the nuclear structure in the form of a Spectroscopic factor (which provides information about the nuclear structure after a nucleon is removed or added to nucleus), and from the nuclear reaction (which as mentioned before is encoded in the optical potential). The issue is that theoretical cross sections have in general been overestimated in comparison to the experimental results in the case of knockout reactions, which might arise from a disparity in the theoretical resolution scale of the structure and reaction components. In this context, the theoretical resolution scale does not refer to the resolution scale set by the kinematics of the experiment, but it is rather set by the maximum momentum components of the potential or wave function being studied. As we need to treat the reaction and structure components at equal resolution, the Similiarity Renormalization Group (SRG) is an invaluable tool, as one could SRG evolve the Optical Potential to a lower resolution to match the scale set by the structure components.

In this project we aim to dissect the effects of the SRG on the optical potential by looking at the simplest reaction - the $d(n,d)n$ transfer reaction. As my current expertise lies in developing SRG methods for analyses of optical potentials, I have existing subroutines that SRG evolve momentum space potentials. However At LLNL there are subroutines in coordinate space that calculate the bound and scattering state wave functions, as well as the T-matrix using the DWBA. In order to use the subroutines at LLNL, we also developed Fourier Transform (FT) codes to transform the existing momentum-space potentials after SRG evolving it so then we can build the optical potential.

As the $d(n,d)n$ reaction does not involve the excitation of the target, the optical potential will not be complex. Nevertheless, we can still observe the effects of the SRG by constructing the folding potential, which integrates (or "folds") the neutron-target and proton-target optical potentials to the bound state of the deuteron [1]. As such, the inputs of our system include a nonlocal NN interaction for the nucleon-target potentials, and the bound-state deuteron wave function. In order to calculate the cross section, we need to construct the T-matrix using the Distorted-Wave Born Approximation (DWBA), using inputs such as the scattering wave function and the optical potential.

The notes are organized as thus: Section II contains the derivations required to build the subroutines for the FT, as well as plots benchmarking the FT does work for a separable nonlocal potential. Section III contains a discussion about the types of potentials used to test the FT and other quantities (such as bound/scattering wave functions) used in the Python subroutines. We also discuss the local and nonlocal folding potential, along with a plot benchmarking the local case. Section IV provides a conclusion and outlook for the project.

II. FOURIER TRANSFORM OF THE NN INTERACTION

As the NN interactions we will be SRG evolving are in momentum-space and in partial waves, we derive the FT expressions for transforming from momentum to coordinate-space in the expression :

$$V(\vec{r},\vec{r}') = \frac{1}{(2\pi)^3}\int d^3k \int d^3k' e^{i\vec{k}\cdot\vec{r}} e^{-i\vec{k}'\cdot\vec{r}'} F(\vec{k},\vec{k}') \tag{1}$$

Here the vectors $\vec{r}$ and $\vec{k}$ correspond to the coordinate and momentum-space vectors, and their primed counterparts correspond to those vectors in different orientations (in coordinate and momentum-space respectively). We have these primed coordinates as we are working with nonlocal NN interactions, which depend on the integral over all space (again either coordinate or momentum-space). Assuming our momentum space potential $F(\vec{k},\vec{k'})$ is central, we can perform the partial-wave expansion on the plane-waves and the momentum-space potential to obtain the following expression for the lth partial wave potential in coordinate-space:

$$v_l(r,r') = \frac{2}{\pi} rr' \int dk \int dk k^2 k'^2 j_l(kr) j_l(k'r') f_l(k,k') \tag{2}$$

where we also expanded the $V(\vec{r},\vec{r}')$ in partial-waves and $v_l(r,r')$ is the lth partial-wave coordinate space potential. The $j_l(kr)$ correspond to the spherical bessel function of order l, and $f_l(k,k')$ is the lth partial-wave momentum-space potential. Also, the FT of the wave-function $\psi_l(\vec{k})$ for the lth partial wave can be expressed as:

$$\psi_l(r) = \sqrt{\frac{2}{\pi}} r \int dk k^2 j_l(kr) \psi_l(k) \tag{3}$$

Similarly, we can derive the inverse FT from coordinate to momentum-space. The corresponding expressions for the partial-wave potential and the wavefunction are:

$$f_l(k,k') = \frac{2}{\pi}\int dr \int drrr' j_l(kr) j_l(k'r') v_l(r,r') \tag{4}$$

and

$$\psi_l(k) = \sqrt{\frac{2}{\pi}} \int drr j_l(kr) \psi_l(r) \tag{5}$$

respectively.

III. POTENTIALS IMPLEMENTED FOR FT AND LLNL SUBROUTINES

To benchmark the different components of our project, such as the FT and the behavior of the wave functions, we worked with several different potentials. We began with a potential that has an analytical form both in coordinate-space and in momentum-space, like the

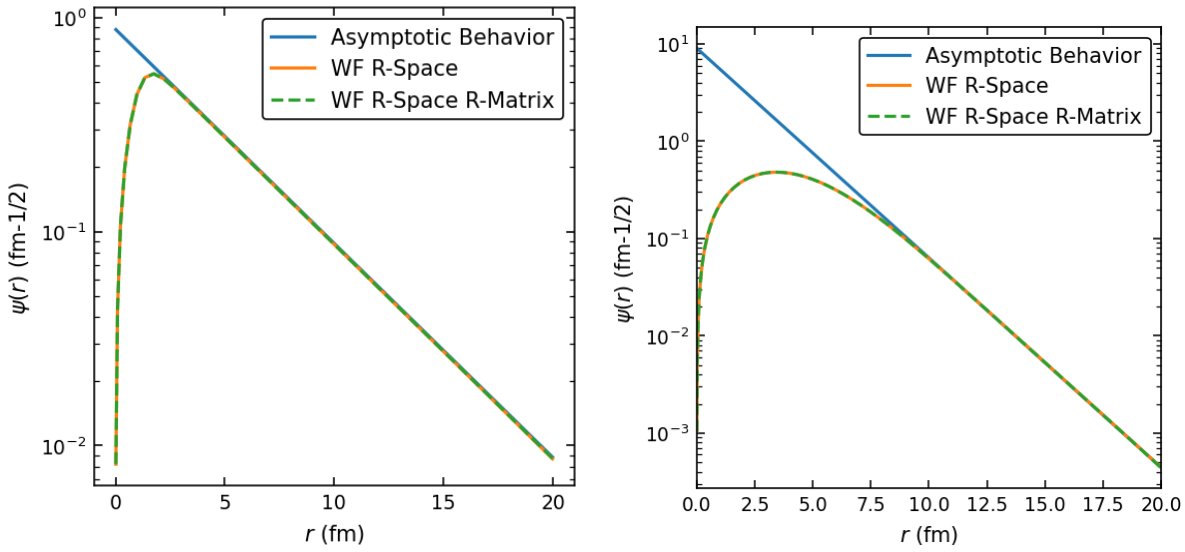

FIG. 1. Left: Minnesota potential. Calculated momentum-space wave-function, then FT it and compared to the wave-function obtained through the R-matrix Right: Nonlocal Separable Potential. Compared FT version of the momentum-space wave-function after obtaining coordinate-space potential by FT the momentum-space one, then calculated wave-function using R-matrix subroutine. Used a Gaussian-Legendre mesh with 40 points, and a channel radius of 20 fm. We compare the asymptotic behavior of the wave function with $e^{-\sqrt{2mE_b}/\hbar}$, where E_b is the binding energy.

Minnesota potential [2], a purely S-wave interaction that reproduces the observables of nuclei by using a sum of three Gaussians, which has the form:

$$V_{minn}(r) = \sum_i^3 V_i e^{-\kappa_i r^2} \tag{6}$$

$$V_{minn}(k,k') = \sqrt{\frac{2}{\kappa}}\frac{1}{kk'}\sum_i^3 V_i(e^{-(k-k')^2/4\kappa_i} - e^{-(k+k')^2/4\kappa_i}) \tag{7}$$

where the strengths V_i have units of MeV and κ has units of fm^2.

To test the subroutines for calculating the bound and scattering state wave functions developed at LLNL, we input the coordinate-space Minnesota potential to check if they return the correct deuteron binding energy (-2.22 MeV), and to see if we can produce plots for the wave-function (both bound and scattering states). In Figure 1 we plot the bound state wave-function of the Minnesota potential using two methods - (1) Take the momentum-space Minnesota potential, calculate the bound state wave-function, and then FT the momentum-space wave-function or (2) Build directly the coordinate-space potential and calculate the wave-function using the LLNL subroutines which uses the R-matrix [3] to calculate the wave-function. As can be seen in Figure 1, the bound state wave-function for both cases has the correct binding energy of -2.22 MeV, and both the FT wave-function and wave-function obtained from the R-matrix code have the same asymptotic behavior, as they are parallel with the $e^{-\sqrt{2mE_b}/\hbar}$ plot, where E_b is the binding energy.

Now to test the LLNL subroutines for a nonlocal potential, we look at first a separable

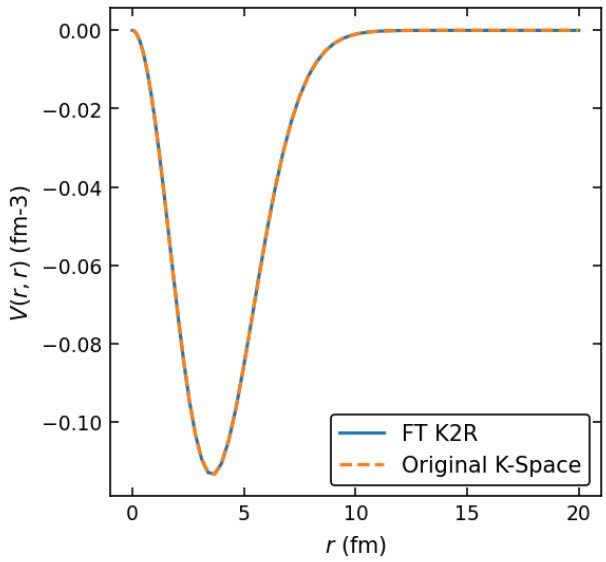

FIG. 2. Diagonal of the coordinate-space separable nonlocal potential. Here we compare the analytical expression vs the FT expression, obtained from the k-space potential. We used 80 points and a channel radius of 20 fm, and had a momentum-space mesh with 50 points and a $k_{max} = 10$ fm.

potential of the form for the $l = 0$ partial wave:

$$v_0(r, r') = \frac{2m}{\hbar^2} V_{0r} r r' e^{-r^2/16} e^{-r'^2/64} \tag{8}$$

$$f_0(k, k') = \frac{2m}{\hbar^2} V_{0k} e^{-4k^2} e^{-16k'^2} \tag{9}$$

where the constants V_{0k} and V_{0r} have units of MeV-fm^3 and MeV-fm^{-3}, which then makes fm^{-3} and fm the units for $v_l(r, r')$ and $f_l(k, k')$.

To benchmark our expressions for the FT, we implement the nonlocal separable potential, and Figure 2 exhibits the agreement the FT subroutine has with the analytical expression for the coordinate-space nonlocal separable potential.

Now taking the FT of $f_0(k, k')$ and passing it through the subroutines for calculating the bound state wavefunction, we reproduced the binding energy (-10.2 MeV) and the $l = 0$ bound state wave-function. It should be noted that for the nonlocal separable potential, we do not reproduce the deuteron binding energy. The purpose of the potential to to test the existing FT and LLNL subroutines. Similar to the Minnesota potential, the wave-function obtained by FT the momentum-space wave-function and from the bound-state wave function obtained by the R-matrix both exhibit the same asymptotic behavior.

In addition to inspecting the bound states, we also looked at the scattering states for each potential, as we want to benchmark the LLNL subroutine for calculating the scattering states and the phase shifts. We do not directly FT the momentum-space scattering wave function as we need the coordinate space NN potentials as inputs for our optical potential which we discuss in Section III A. For both potentials, we looked at 100 MeV scattering energies, and plotted them in Figure 3. We find that both wave-functions have similar asymptotic behavior, as they are agree well with the $l = 0$ spherical Bessel function $J_0(kr)$.

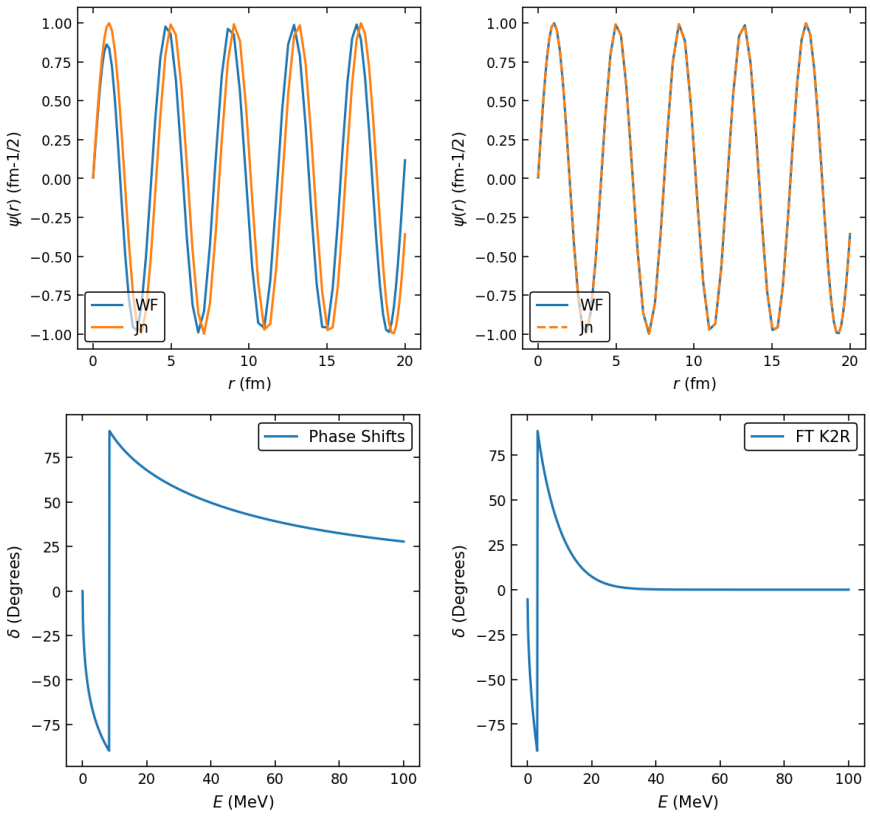

FIG. 3. Coordinate-space scattering wave-function (top) and phase shifts (bottom) of the Minnesota (left column) and separable (right column) potentials at 100 MeV. We compare it with the asymptotic form aka a spherical bessel function of order zero $J_0(kr)$. We used a Gaussian-Legendre mesh with 80 points, and a channel radius of 20 fm and a k-space mesh with 100 points and a k_{max} of $10 fm^{-1}$.

In the case of the Minnesota potential, we see a small phase shift for the scattering states at 100 MeV, which corresponded to a small shift in the scattering wave function in comparison to $J_0(kr)$. However, as the phase shift for the nonlocal separable potential was zero, there is no shift in the scattering wave function.

A. Watanabe Folding Potential

To model the $d(n,d)n$ reaction, we consider a three-body Hamiltonian:

$$H = T_1 + T_2 + V_{12}(r) + V_1(r_1) + V_2(r_2), \tag{10}$$

from which we build an effective deuteron-nucleus potential by implementing the folding potential as prescribed by Watanabe in his seminal paper. This potential is built upon the interaction between the proton and the target neutron ($V_1(r_1)$), and corresponding interaction with the deuteron's neutron and the nucleus ($V_2(r_2)$), and finally the interaction between the proton and neutron within the deuteron ($V_{12}(r)$, where $r = |\vec{r}_1 - \vec{r}_2|$) The terms $T_1 = \frac{\hbar^2}{2m}\nabla_1^2$ and $T_2 = \frac{\hbar^2}{2m}\nabla_2^2$ correspond to the kinetic energies of the neutron and proton, respectively. Incorporating the center of mass $\vec{R} = \frac{1}{2}(\vec{r}_1 + \vec{r}_2)$ and relative coordinates

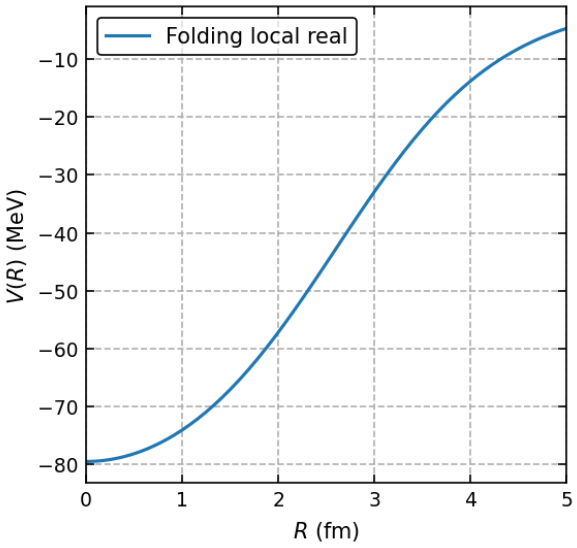

FIG. 4. Coordinate-space local folding potential, with a Woods-Saxon potential for the NN interaction, and a Hulthen wave-function. The strength of the potential is 50 MeV, with A=10, a=.65 fm.

$\vec{r} = \vec{r}_1 - \vec{r}_2$, we express $\vec{r}_1$ and $\vec{r}_2$ as $\vec{r}_1 = \vec{R} + \frac{\vec{r}}{2}$ and $\vec{r}_2 = \vec{R} - \frac{\vec{r}}{2}$. We then factorize the deuteron wave function into its relative and center-of-mass components, and insert it into the three-body Hamiltonian. We then express the folding potential as:

$$V(R) = \int d\vec{r}\chi(\vec{r})(V_1(|\vec{R} + \frac{\vec{r}}{2}|) + V_2(|\vec{R} - \frac{\vec{r}}{2}|))\chi(\vec{r}) \tag{11}$$

Now we can apply a partial-wave expansion on the deuteron bound state wave function $\chi(\vec{r})$ and the interactions $V_1(|\vec{R} + \frac{\vec{r}}{2}|)$ and $V_2(|\vec{R} - \frac{\vec{r}}{2}|)$, which will eventually lead us to:

$$V(R) = \frac{1}{4\pi}\sum_{i,l}\int dr\chi_l(r)W_{li}(r_i)\chi_l(r) \tag{12}$$

Here the sum over i corresponds to the neutron-target and proton-target interactions, for which we used the partial-wave expansion on the deuteron-nucleon potentials $V_i(r_i)$. Using the orthogonality of the spherical harmonics $Y_l(\Omega_r)$, we can isolate $W_{li}(r_i)$ and as the deuteron optical potential is central in R only the monopole term ($l = 0$) in the partial-wave expansion in nonzero, giving us $W_{0i}(r_i) = \frac{1}{2}\int d\theta sin(\theta)V_i(r_i)$.

In Figure 4 we plot the local folding potential using a Hulthen wave function. We also use a Woods-Saxon potential for the NN interaction, and the parameters for the wave function and the Woods-Saxon potential are given in [4], which we use to benchmark our local folding potential expression (12).

We can do a similar derivation of the nonlocal folding potential and expand in partial waves the individual components as in the local case to obtain:

$$V(\vec{R}, \vec{R}') = \sum_i\sum_l \frac{1}{4\pi}P_l(cos(\theta_R))\int drdr'rr'\chi_l(r')\chi_l(r)u_{l,i}(r, R, r', R') \tag{13}$$

where θ_R is the angle between $\vec{R}$ and $\vec{R}'$ And $u_{l,i}(r, R, r', R')$ is defined as:

$$u_{l,i}(r, R, r', R') = \frac{2l+1}{4} \int d\theta_{r,R} d\theta_{r',R'} sin(\theta_{r,R}) sin(\theta_{r',R'}) V_i(r, R, r', R') P_l(cos(\theta_{r,R})) P_l(cos(\theta_{r',R'})) \tag{14}$$

where $\theta_{r,R}$ represents the angle between $\vec{r}$ and $\vec{R}$ (similarly for the primed coordinates).

IV. CONCLUSION

Optical potentials are a powerful tool to describe nuclear reactions within the scope of a single expression, which reduces the many-body problem to a few-body one. Coupling optical potentials with SRG will allow us to calculate cross sections in a systematic manner, with the overall goal to obtain more accurate calculations for such cross sections.

In this study we begin the process of studying optical potentials by building our own FT subroutines in order to interface with my current SRG codes in momentum-space with the coordinate-space codes developed at LLNL for calculating the bound/scattering states and the T-matrix. We have checked that the FT subroutines work for a nonlocal separable potential, and that the LLNL subroutines return the correct bound/scattering states by FT the momentum space wave function and benchmarking it by looking at the asymptotic conditions for the bound/scattering states.

We then started constructing the folding potential, where the nucleon-target potentials that serve as inputs to the folding potential are currently being taken as Woods-Saxon potentials to benchmark the current subroutines for the folding potential. As of now we developed the local folding potential with the aforementioned Woods-Saxon potential and using a Hulthen wave function. After benchmarking the nonlocal folding potential, we intend to use more involved NN interactions that are also nonlocal, such as the AV18 potential (and use the corresponding wave functions).

In the future we will implement the nonlocal folding potential, for which we will SRG evolve the NN interaction itself, then FT the interaction. The corresponding evolved coordinate-space NN interaction will be used to build the deuteron-nucleon optical potential at each SRG resolution scale, which will allow us to explore the scale-dependence of the certain aspects of the optical potential in the context of $d(n, d)n$ reactions, such as nonlocality. In addition, we want to explore the behaviors of the T-matrix, which will be used to calculate the cross section, as we SRG evolve the NN interaction.

[1] S. Watanabe, Nucl. Phys. **8**, 484 (1958).

[2] D. R. Thompson, M. Lemere, and Y. C. Tang, Nucl. Phys. A **286**, 53 (1977).

[3] P. Descouvemont and D. Baye, Rept. Prog. Phys. **73**, 036301 (2010), arXiv:1001.0678 [nucl-th].

[4] F. G. Perey and G. R. Satchler, Nucl. Phys. A **97**, 515 (1967).